

See discussions, stats, and author profiles for this publication at: <https://www.researchgate.net/publication/5246594>

Innovative Solid-State Microelectrode for Nitrite Determination in a Nitrifying Granule

ARTICLE *in* ENVIRONMENTAL SCIENCE AND TECHNOLOGY · JULY 2008

Impact Factor: 5.33 · DOI: 10.1021/es800409s · Source: PubMed

CITATIONS

6

READS

18

9 AUTHORS, INCLUDING:



Shaoyang Liu

Troy University

26 PUBLICATIONS 318 CITATIONS

[SEE PROFILE](#)



Gang Liu

University of Science and Technology of C...

84 PUBLICATIONS 1,014 CITATIONS

[SEE PROFILE](#)



Han-Qing Yu

University of Science and Technology of C...

508 PUBLICATIONS 11,050 CITATIONS

[SEE PROFILE](#)

Innovative Solid-State Microelectrode for Nitrite Determination in a Nitrifying Granule

SHAO-YANG LIU,[†] YOU-PENG CHEN,[†]
FANG FANG,[†] SHU-HONG LI,[†]
BING-JIE NI,[†] GANG LIU,[‡]
YANG-CHAO TIAN,[‡] YING XIONG,[‡] AND
HAN-QING YU^{*,†}

Department of Chemistry and National Synchrotron Radiation Laboratory, University of Science & Technology of China, Hefei 230026, China

Received October 03, 2007. Revised manuscript received March 10, 2008. Accepted April 08, 2008.

Nitrite is an intermediate of both nitrification and denitrification in biological removal of nitrogen from wastewater, and in situ measurement of nitrite concentration in a biofilm or microbial granules is highly desirable. However, a solid-state microelectrode for nitrite determination is not available yet. In this work, a solid-state microelectrode was manufactured through electrochemical codeposition of Pt–Fe nanoparticles on a gold microelectrode fabricated using photolithography for in situ nitrite determination. This gold-based microelectrode could be used as a more cost-effective, efficient, and reliable alternative to the liquid membrane microelectrode. Nanoparticles with an average diameter of 50 nm were observed on the surface of the chemically modified electrode. A sigmoid peak at ca. 0.7 V (vs Ag/AgCl) was found on the linear sweep voltammogram in nitrite solutions by using the fabricated microelectrode. The peak height of the first-order derivative of the sigmoid peak was proportional to the nitrite concentration of 0.001–0.05 M and could be used for quantitative determination of nitrite. The detection limits ($S/N = 3$) were approximately 3×10^{-5} M. The nitrite microprofiles of aerobic granules from a nitrifying reactor were measured with the microelectrode to demonstrate its potential applications with high spatial resolution.

Introduction

Nitrite is an intermediate of both nitrification and denitrification, the two essential processes in biological nitrogen removal (BNR) for wastewater treatment (1–5). In many cases nitrite may build up at a considerable concentration in bioreactors. For example, when the nitrification capacity of activated sludge in reactors has been undersized or is not functioning properly, nitrite may accumulate. Moreover, nitrite plays an even more important role in a number of novel BNR processes (6), such as the short-cut nitrification and denitrification process (7), completely autotrophic nitrogen removal over nitrite process (8), and oxygen-limited autotrophic nitrification–denitrification process (3). On the other hand, a biofilm and aerobic granules have been used in BNR processes. In this case, oxygen diffusion limitation

may cause both aerobic and anoxic microenvironments in the biofilm or granules, allowing sequential utilization of electron acceptors such as oxygen, nitrite, and nitrate. Furthermore, since nitrite is an intermediate in BNR processes, its presence could be temporary. Thus, in situ measurement of nitrite concentrations in the biofilm or granules becomes crucial to elucidate and understand the nitrogen removal mechanisms by the microbial species. Therefore, the determination of the nitrite distribution in biofilms or granules is highly desirable.

Many analytical methods have been developed for the measurement of nitrite (9), but most of them are not applicable to biofilms or microbial granules. A microelectrode is appropriate for this objective. A selective liquid ion-exchanging membrane nitrite microelectrode has been developed with a hydrophobic ion carrier, aquocyanocobalt(III) hepta(2-phenylethyl)cobrylate (10). The nitrite microelectrode showed a log-linear response to nitrite concentration and has been applied in investigations into biofilms (7, 11) and sediments (12, 13). However, the lifetime of the liquid ion-exchanging membrane microelectrode is short, and it is not easy to obtain an appropriate ion carrier.

In our previous work, a solid-state gold microelectrode was successfully fabricated using photolithography and used to measure the dissolved oxygen (DO) microprofiles in aerobic granules (14). Gold was selected as the electrode material as it could be used to measure DO directly (15) and has a great functionalizing potential to monitor a large number of other environmental factors, e.g., glucose (16) and nucleic acid (17). Such a solid-state gold microelectrode would also be able to measure nitrite after a proper functionalization.

Chemical modification is a powerful method for electrode functionalization (18, 19) and is widely used in determination of SO_2 (20), pH (21), carbohydrates (22), and human serum albumin (23). Chemically modified electrodes (CMEs) with good catalytic activity toward the oxidation of nitrite anions could be used for nitrite determination. A thin film of mixed-valence CuPtCl_6 was electrochemically deposited on a glassy carbon electrode (GCE) and applied in a flow-injection system for nitrite measurement (24). Recently, the use of metal nanoparticle superstructures for electrochemical sensing devices has attracted increasing interest (25, 26). A CME from electrochemical codeposition of Pt nanoparticles and Fe(III) on a GCE showed a quantitative response to nitrite (27).

In the present work a nitrite microelectrode was manufactured through electrochemical codeposition of Pt–Fe nanoparticles on our solid-state gold microelectrode fabricated using photolithography to provide a more cost-effective and efficient alternative to the liquid membrane microelectrode for in situ nitrite measurement. The performance of the fabricated microelectrode for nitrite determination was evaluated. The nitrite and DO distributions in aerobic granules from a nitrifying bioreactor were measured with this microelectrode.

Experimental Section

Chemicals. Potassium ferricyanide, potassium ferrocyanide, potassium chloride, sodium nitrite, ferric trichloride, and hexachloroplatinic acid, all purchased from Shanghai Chemical Reagent Co., were of analytical grade and used as received. Deionized water was used throughout the experiments.

Apparatus. All electrochemical experiments including cyclic voltammetry (CV), linear sweep voltammetry (LSV), and chronoamperometry were performed using an electrochemical detector (CHI 800, CH Instruments Inc.) at 25 °C.

* Corresponding author. fax: +86 551 3601592; e-mail: hqyu@ustc.edu.cn.

[†] Department of Chemistry.

[‡] National Synchrotron Radiation Laboratory.

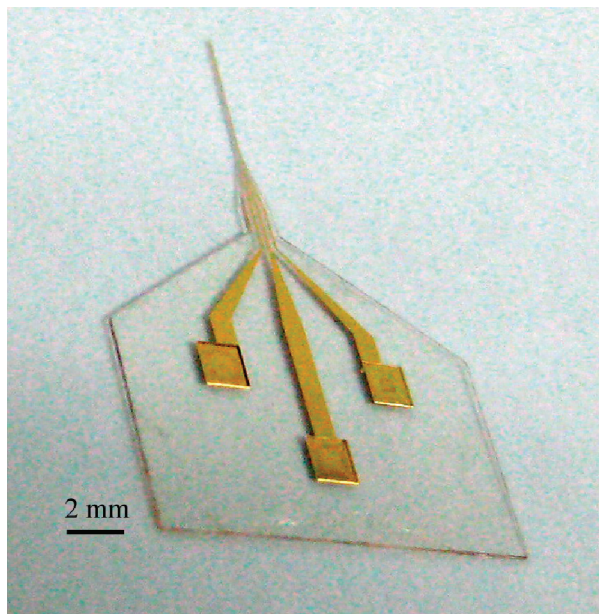


FIGURE 1. Image of the novel gold microelectrode.

A three-electrode configuration was employed. A commercial Ag/AgCl electrode (CHI111, CH Instruments Inc.) was used as the reference. A platinum wire counterelectrode (CHI115, CH Instruments Inc.) was used for electrochemical modification. LSV experiments were performed at a scan rate of 50 mV/s. A scan from 0.4 to 1.0 V was completed in 12 s. A scanning electron microscopy (SEM) image was obtained on a nanoengineering workstation (e-LINE, Raith Co., Germany).

Preparation of the CME. A novel microelectrode fabricated using photolithography was used for electrochemical modification (Figure 1). The microelectrode fabrication procedures have been reported previously (14), and they thus are only described here briefly: (i) photopatterning the microelectrode shape onto a 50 μm layer of SU-8 spin-coated on a glass substrate, (ii) sputtering deposition of a thin layer of titanium and a 500 nm layer of gold, (iii) photolithographic definition of metal tracks onto a positive photoresist layer on the gold layer, (iv) ion beam etching to remove the uncovered metal, (v) photopatterning the microelectrode shape and external contact pads onto the upper 50 μm layer of SU-8, (vi) developing SU-8 and detaching the microelectrode from the glass substrate, (vii) attaching copper wires to the contact pads with silver conductive paint and insulating the pads with silicon rubber.

The microelectrode had a small needle of 70 μm width, 100 μm thickness, and 5 mm length on which two working microelectrodes and a counterelectrode were integrated. Prior to use, the needle tip was severed with a sharp knife to reveal the cross-sections of the gold tracks of the two working electrodes as active surfaces. One side of the golden surface was located at the center of the needle cross-section, and the other side was next to it with an internal length of 10 μm . The nominal shape of the golden surface was a rectangle (0.5 μm \times 10 μm), but its actual shape depended on the fabrication and cutting procedures. The needle, which provides sufficient space to contain the three electrodes and sufficient mechanical strength to insert into samples, is bigger than that of the usual microelectrodes commonly used for measurement of microbial aggregates. This microelectrode may create a channel through which surface liquids can flow, thus contaminating a granule or a biofilm being measured. Thus, a more precise photolithography technique and photoresistants with better mechanical characteristics should be used

to reduce the size of the microelectrode and increase its measurement accuracy in the future.

The modification of the gold working electrode was accomplished with a cyclic voltammetry scan between +0.75 and -0.30 V at a scan rate of 50 mV/s for 30 cycles in a deposition solution, which was composed of 1.8×10^{-3} M H₂PtCl₆, 1.2×10^{-3} M FeCl₃, and 1.0 M KCl. Then the CME was rinsed with water and conditioned in 0.2 M KCl overnight. After rinsing again and air drying, the microelectrode tip was dipped in a solution of 12% cellulose acetate in acetone as rapidly as possible to coat a thin cellulose acetate film on it.

Nitrite and DO Microprofile Measurements of a Nitrifying Granule. A column-type sequencing batch reactor (SBR) was used to cultivate nitrifying granules as described previously (14). When the nitrifying granules were sampled, the synthetic wastewater was composed as follows (concentration, mM): NH₄Cl (3.74), K₂HPO₄ (0.23), CaCl₂ (0.090), MgCl₂·6H₂O (0.025), FeSO₄·7H₂O (0.015). The pH was kept in a range of 7.0–8.5 through a dose of NaHCO₃.

Nitrifying granules (Figure 2A) with a diameter of 3 mm and a solution in the SBR were sampled at the end of the operating cycle for microprofile measurements. The bulk solution drawn from the SBR contained NH₄⁺ (N concentration of 2.4 mM), NO₂⁻ (N concentration of 6.1 mM), and NO₃⁻ (N concentration of 1.2 mM). Most of the NH₄⁺ in the influent was converted into NO₂⁻ at the end of the operation cycle. The solution was immediately transferred to a test chamber (Figure 2B), and a granule was carefully settled on the nylon net. Then the granule was cultivated over 1 h prior to the test to achieve a pseudo steady state. During the profile measurement, a micromanipulator was used to adjust the position of the microelectrode tip at a spatial resolution of 5 μm and a microscope was used for precisely locating the granular surface. The movement of the microelectrode tip was perpendicular to the granular surface (Figure 2C,D). No buckling of the needle and no significant changes of the granule were observed in the measurement.

The two working electrodes at the microelectrode tip were respectively used to measure DO and nitrite microprofiles. One unmodified working gold electrode with a thin cellulose acetate film was employed to measure the DO distribution in the granule by using chronoamperometry. The cathode was polarized at -0.75 V (vs Ag/AgCl), and the limiting current was proportional to the DO level (14, 28). Its calibrations were performed in the bulk solution before and after the measurements with a DO sensor (MO128, Mettler-Toledo GmbH, Switzerland). Another CME was employed for nitrite measurement and was also calibrated in the bulk solution before and after the measurement. The changes of the responses were less than 10%.

Results and Discussion

Chemical Modification of the Microelectrode. Figure 3 shows the typical cyclic voltammograms of the electrochemical codeposition process of Pt–Fe nanoparticles on the gold-based working electrode. Three redox couples were observed, which corresponded to Fe³⁺/Fe²⁺ (I), PtCl₆⁴⁻/PtCl₄²⁻ (II), and PtCl₄²⁻/Pt⁰ (III) respectively (29, 30). The peak currents gradually increased with the scan number, indicating the accumulation of the modifier on the electrode surface. The SEM image of the surface of the CME is illustrated in Figure 4. Pt–Fe particles with an average diameter of about 50 nm were observed to distribute on the electrode surface.

Pt–Fe nanoparticles could be readily codeposited on a GCE with a diameter of 4 mm using cyclic voltammetry (27). However, the functionalizing method had to be modified to finalize a codeposition of Pt–Fe nanoparticles on a small-sized microelectrode. The microelectrode could be damaged by a low negative potential, because the SU8, a negative photoresist used as an insulating and supporting material

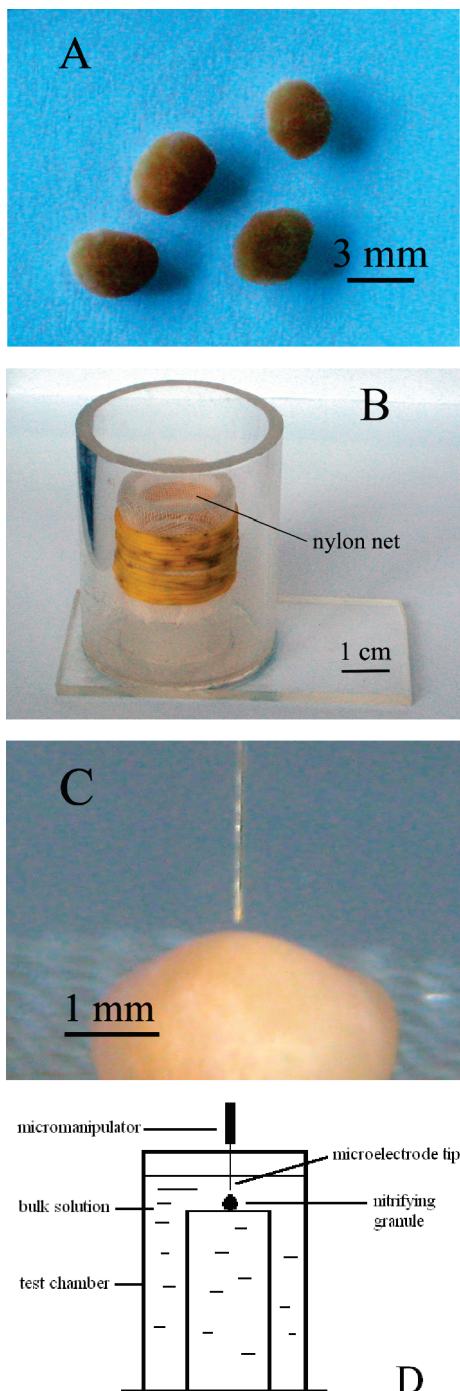


FIGURE 2. Images of the (A) nitrifying granules tested, (B) test chamber used for DO and NO_2^- micropore measurement, and (C) measurement process and (D) schematic diagram of micropore monitoring.

in the microelectrode, is readily deteriorated when exposed to a low negative potential. The lower end of the scan range of potential should be as high as possible to accomplish the codeposition. Thus, a potential of -0.3 V (vs Ag/AgCl) was selected in this work. The CME response was not stable in 0.2 M KCl solution, especially after it had been used several times or exposed to biological samples. This might be attributed to the small electrode surface, on which a slight change would cause a notable response shift. A thin cellulose acetate film was used to sort out this problem, as it could protect the CME and reduce the effects of biological samples.

Cyclic voltammograms of the same working electrode in the modification process in a solution with 0.005 M ferro/

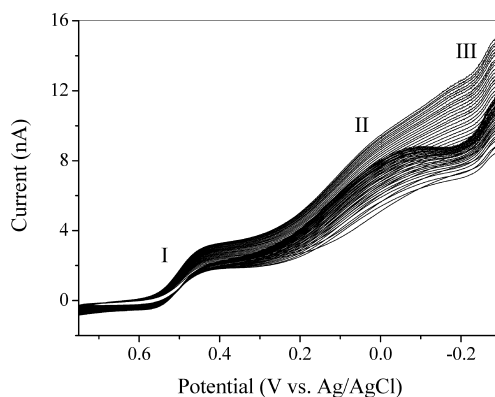


FIGURE 3. Cyclic voltammetry of the electrodeposition process in a solution containing 1.8×10^{-3} M H_2PtCl_6 , 1.2×10^{-3} M FeCl_3 , and 1.0 M KCl between $+0.75$ and -0.30 V at a scan rate of 50 mV/s.

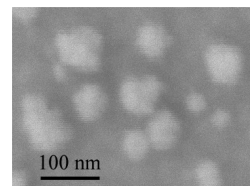


FIGURE 4. SEM image of the surface of the electrochemically modified working electrode.

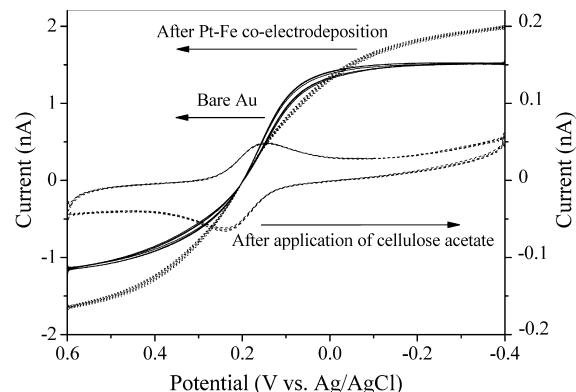


FIGURE 5. Cyclic voltammograms of the same working electrode in the modification in 0.005 M ferro/ferricyanide and 0.1 M KCl solution at a scan rate of 0.1 V/s (three circles were recorded).

ferricyanide and 0.1 M KCl are shown in Figure 5. After the coelectrodeposition of Pt–Fe, the peak currents of the voltammogram increased with a small shape transformation, suggesting that the electrochemical property of the working electrode was changed and became more active. After utilization of the thin cellulose acetate film, the peak currents decreased significantly. The anodic and cathodic waves were separated, and their shapes were shifted from sigmoid type toward peak type. This was attributed to the diffusion limitation caused by the cellulose acetate film. All three voltammograms were stable and reversible, demonstrating that the working electrode was reliable in the modification process.

Performance of the CME for Nitrite Determination. Linear sweep voltammograms of the same working electrode before and after the electrochemical modification in 0.005 M NaNO_2 solution at a scan rate of 50 mV/s were essentially different (Figure 6). Before the modification, no evident peak was found in the voltammogram. However, after the electrochemical codeposition, a clear sigmoid peak appeared at 0.7 V and could be used for quantitative determination of

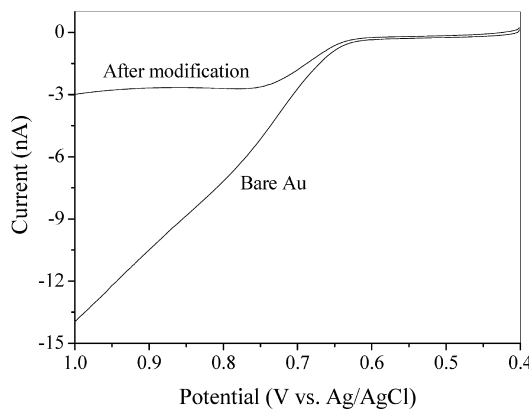


FIGURE 6. Linear sweep voltammograms of the same working electrode before and after the electrochemical modification in 0.005 M NaNO₂ solution at a scan rate of 50 mV/s.

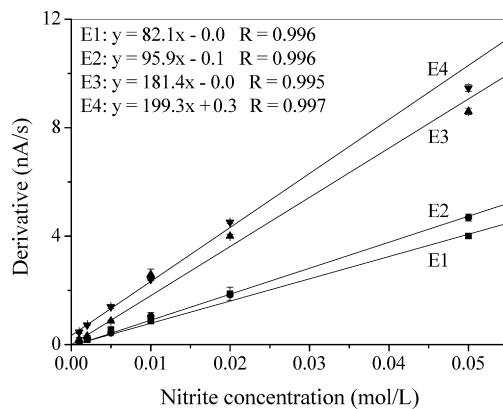


FIGURE 7. Calibration curves of four independent CMEs at a scan rate of 50 mV/s.

nitrite. Such a change should be attributed to the catalytic activity toward the NO₂⁻ oxidation of the deposited particles on the gold electrode surface. Therefore, gold microelectrodes could be modified by using the method proposed in this work for NO₂⁻ measurement.

Chemical modifications were also performed in the absence of FeCl₃ or H₂PtCl₆ in the deposition solution. The response of the CME fabricated in the absence of FeCl₃ to nitrite was substantially reduced, and the CME formed in the absence of H₂PtCl₆ had no response to nitrite at all. This confirms that the nanoparticles on CME were composed of both Pt and Fe and suggests that Pt and Fe had a coordinated effect on the catalytic oxidation of nitrite.

The peak height of the first-order derivative curve of the linear sweep voltammogram was used for quantitative determination of nitrite, which showed a better anti-interference ability than the height of the sigmoid peak of the linear sweep voltammogram. Calibration curves of four independent CMEs are illustrated in Figure 7. Linear dependence of the peak height of the derivative curve on the nitrite concentration was observed, and high correlation coefficients were found in each case. The response of NO₂⁻ ranged from 82.1 to 199.3 (nA/s)/(mol/L). This was likely to be attributed to the differences originating from the micro-fabrication, severing, and electrochemical modification processes. The detection limit (S/N = 3) was appropriately 3×10^{-5} M. The nitrite microelectrode was not as sensitive as the usually sized electrodes reported (24, 27). This is probably associated with the limited active surface of the microelectrode. Although such a sensitivity is acceptable to be used for the measurement of aerobic granules in the field of wastewater treatment, a lower detection limit is required

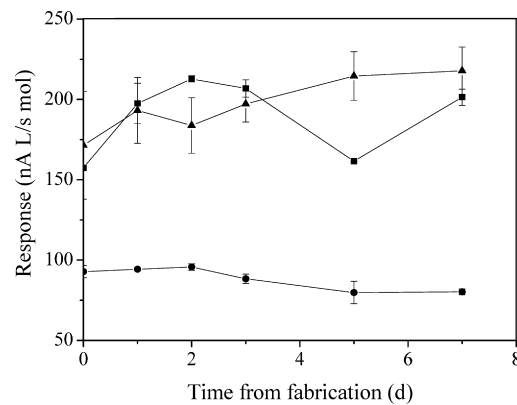


FIGURE 8. Lifetimes of three independent CMEs stored in water.

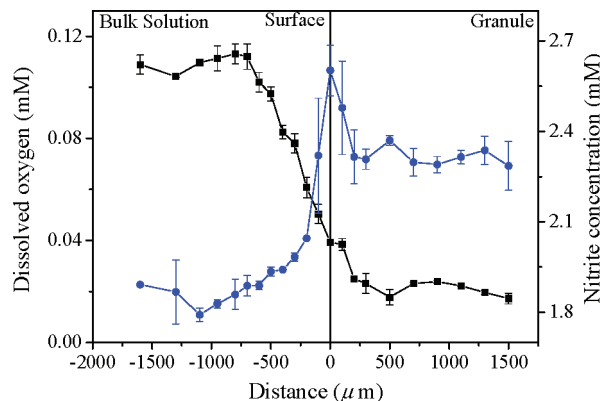


FIGURE 9. Nitrite and DO microprofiles in a granule. Point 0 on the x axis indicates the granular surface. Negative depth values (to the left of zero) were in the bulk, and positive depth values (right of zero) were in the granule.

for other applications. Thus, a better functionalizing method and optimizing fabrication conditions should be explored.

When the CME was stored in air, its response to NO₂ was lost in two days. However, if the electrode tip was kept in water, the CME worked for over a week, as shown in Figure 8.

The anti-interference ability of the CME was also investigated. The interferences of Mg²⁺, Fe³⁺, and Zn²⁺ at 50 mg/L, Cu²⁺, NH₄⁺, and NO₃⁻ at 150 mg/L, and Cl⁻, Na⁺, and SO₄²⁻ at 200 mg/L were small (<5%) in the determination of 0.005 M NO₂⁻. In addition, the ion strength (0.02–0.09 mol/kg) and pH (6.0–8.0) had no significant effect on the CME response (data not shown).

Nitrite and DO Distributions in a Nitrifying Granule. The measured nitrite and DO distributions in a nitrifying granule are illustrated in Figure 9. Point 0 on the x axis indicates the granular surface. The DO level in the bulk solution for the nitrite and DO distribution measurement was approximately 1.1 mM. In the upper layer of the granule with a thickness of ca. 200 μm, the highest nitrite concentrations were observed coupled with a rapid DO drop, indicating that most of the active ammonia-oxidizing bacteria (AOB) were aggregated in this layer. In the inner part of the granule, the DO level decreased gradually and the nitrite concentration was lower than that in the upper layer. The nitrite was converted into nitrate by the nitrite-oxidizing bacteria (NOB) with a consumption of DO. Since the DO decreasing rate was slow, the abundance of the NOB in the inner part should be low. No oxygen depletion zone was found in the granule, suggesting that the denitrification processes should be insignificant under the tested conditions. At the outside of the granular surface, the nitrite concentration dropped

rapidly because of its diffusion from the granular surface to the bulk solution.

Similar distributions of the AOB and NOB were observed in an autotrophic nitrifying biofilm (11), but the nitrite and DO microprofiles were different. The nitrite concentration decreased monotonically from the bulk solution into the biofilm, and oxygen only penetrated ca. 150 μm into the biofilm. Such a difference might be attributed to the low NH_4^+ N concentration (<0.36 mM) and rapid DO consumption in the biofilm cultivation (11).

Acknowledgments

We thank the Natural Science Foundation of China (Grants 20577048, 50625825, and 50738006), the National Synchrotron Radiation Laboratory, and the Shanghai Tongji Gao Ting-Yao Environment Development Foundation for partial support of this study.

Literature Cited

- (1) Chung, J.; Bae, W.; Lee, Y. W.; Rittmann, B. E. Shortcut biological nitrogen removal in hybrid biofilm/suspended growth reactors. *Process Biochem.* **2007**, *42*, 320–328.
- (2) Gieseke, A.; Tarre, S.; Green, M.; de Beer, D. Nitrification in a biofilm at low pH values: Role of in situ microenvironments and acid tolerance. *Appl. Environ. Microbiol.* **2006**, *72*, 4283–4292.
- (3) Pynaert, K.; Smets, B.; Beheydt, D.; Verstraete, W. Start-up of autotrophic nitrogen removal reactors via sequential biocatalyst addition. *Environ. Sci. Technol.* **2004**, *38*, 1228–1235.
- (4) Satoh, H.; Ono, H.; Rulin, B.; Kamo, J.; Okabe, S.; Fukushi, K. I. Macroscale and microscale analyses of nitrification and denitrification in biofilms attached on membrane aerated Biofilm reactors. *Water Res.* **2004**, *38*, 1633–1641.
- (5) Harms, G.; Layton, A. C.; Dionisi, H. M.; Gregory, I. R.; Garrett, V. M.; Hawkins, S. A.; Robinson, K. G.; Sayler, G. S. Real-time PCR quantification of nitrifying bacteria in a municipal wastewater treatment plant. *Environ. Sci. Technol.* **2003**, *37*, 343–351.
- (6) Schmidt, I.; Slieliers, O.; Schmid, M.; Bock, E.; Fuerst, J.; Kuenen, J. G.; Jetten, M. S. M.; Strous, M. New concepts of microbial treatment processes for the nitrogen removal in wastewater. *FEMS Microbiol. Rev.* **2003**, *27*, 481–492.
- (7) Terada, A.; Lackner, S.; Tsuneda, S.; Smets, B. F. Redox-stratification controlled biofilm (ReSCoBi) for completely autotrophic nitrogen removal: The effect of co- versus counter-diffusion on reactor performance. *Biotechnol. Bioeng.* **2007**, *97*, 40–51.
- (8) Third, K. A.; Paxman, J.; Schmid, M.; Strous, M.; Jetten, M. S. M.; Cord-Ruwisch, R. Treatment of nitrogen-rich wastewater using partial nitrification and Anammox in the CANON process. *Water Sci. Technol.* **2005**, *52*, 47–54.
- (9) Moorcroft, M. J.; Davis, J.; Compton, R. G. Detection and determination of nitrate and nitrite: a review. *Talanta* **2001**, *54*, 785–803.
- (10) de Beer, D.; Schramm, A.; Santegoeds, C. M.; Kuhl, M. A nitrite microsensor for profiling environmental biofilms. *Appl. Environ. Microbiol.* **1997**, *63*, 973–977.
- (11) Okabe, S.; Kindaichi, T.; Ito, T.; Satoh, H. Analysis of size distribution and areal cell density of ammonia-oxidizing bacterial microcolonies in relation to substrate microprofiles in biofilms. *Biotechnol. Bioeng.* **2004**, *85*, 86–95.
- (12) Meyer, R. L.; Risgaard-Petersen, N.; Allen, D. E. Correlation between anammox activity and microscale distribution of nitrite in a subtropical mangrove sediment. *Appl. Environ. Microbiol.* **2005**, *71*, 6142–6149.
- (13) Satoh, H.; Nakamura, Y.; Okabe, S. Influences of infaunal burrows on the community structure and activity of ammonia-oxidizing bacteria in intertidal sediments. *Appl. Environ. Microbiol.* **2007**, *73*, 1341–1348.
- (14) Liu, S.-Y.; Liu, G.; Tian, Y.-C.; Chen, Y.-P.; Yu, H.-Q.; Fang, F. An innovative microelectrode fabricated using photolithography for measuring dissolved oxygen distributions in aerobic granules. *Environ. Sci. Technol.* **2007**, *41*, 5447–5452.
- (15) Linsenmeier, R. A.; Yancey, C. M. Improved fabrication of double-barreled recessed cathode O_2 microelectrodes. *J. Appl. Physiol.* **1987**, *63*, 2554–2557.
- (16) McRiley, M. A.; Linsenmeier, R. A. Fabrication of a mediated glucose oxidase recessed microelectrode for the amperometric determination of glucose. *J. Electroanal. Chem.* **1996**, *414*, 235–246.
- (17) Goral, V. N.; Zaytseva, N. V.; Baeumner, A. J. Electrochemical microfluidic biosensor for the detection of nucleic acid sequences. *Lab Chip* **2006**, *6*, 414–421.
- (18) Murray, R. W. In *Electroanalytical Chemistry*; Bard, A. J., Ed.; Marcel Dekker: New York, 1984; Vol. 13, pp 191–368.
- (19) Wrighton, M. S. Surface functionalization of electrodes with molecular reagents. *Science* **1986**, *231*, 32–37.
- (20) Chiou, C.-Y.; Chou, T.-C. Amperometric sulfur dioxide sensors using the gold deposited gas-diffusion. *Electroanalysis* **1996**, *8*, 1179–1182.
- (21) Bezbarua, A. N.; Zhang, T. C. Fabrication of anodically electrodeposited iridium oxide film ph microelectrodes for microenvironmental studies. *Anal. Chem.* **2002**, *74*, 5726–5733.
- (22) Casella, I. G.; Destradiis, A.; Desimoni, E. Colloidal gold supported onto glassy carbon substrates as an amperometric sensor for carbohydrates in flow injection and liquid chromatography. *Analyst* **1996**, *121*, 249–254.
- (23) Kim, J.-H.; Cho, J.-H.; Cha, G. S.; Lee, C.-W.; Kim, H.-B.; Paek, S.-H. Conductimetric membrane strip immunosensor with polyaniline-bound gold colloids as signal generator. *Biosens. Bioelectron.* **2000**, *14*, 907–915.
- (24) Pei, J.; Li, X. Electrochemical study and flow-injection amperometric detection of trace NO_2^- at CuPtCl_6 chemically modified electrode. *Talanta* **2000**, *51*, 1107–1115.
- (25) Hernandez-Santos, D.; Gonzalez-Garcia, M. B.; Garcia, A. C. Metal-nanoparticles based electroanalysis. *Electroanalysis* **2002**, *14*, 1225–1235.
- (26) Katz, E.; Willner, I.; Wang, J. Electroanalytical and bioelectroanalytical systems based on metal and semiconductor nanoparticles. *Electroanalysis* **2004**, *16*, 19–44.
- (27) Wang, S. Q.; Yin, Y. M.; Lin, X. Q. Cooperative effect of Pt nanoparticles and Fe(III) in the electrocatalytic oxidation of nitrite. *Electrochim. Commun.* **2004**, *6*, 259–262.
- (28) Revsbech, N. P.; Ward, D. M. Oxygen microelectrode that is insensitive to medium chemical composition: use in an acid microbial mat dominated by cyanidium caldarium. *Appl. Environ. Microbiol.* **1983**, *45*, 755–759.
- (29) Humphrey, B. D.; Sinha, S.; Bocarsly, A. B. Mechanisms of charge transfer at the chemically derivatized interface: the $\text{Ni}/[\text{Ni}^{II}(\text{C}-\text{N})\text{Fe}^{II/III}(\text{CN})_5]^{2-/-}$ system as an electrocatalyst. *J. Phys. Chem.* **1987**, *91*, 586–593.
- (30) Xian, Y.; Zhang, W.; Xue, J.; Ying, X.; Jin, L.; Jin, J. Measurement of nitric oxide released in the rat heart with an amperometric microsensor. *Analyst* **2000**, *125*, 1435–1439.

ES800409S